Nuclear Medicine and Biology 41 (2014) 259–267

Contents lists available at ScienceDirect

Nuclear Medicine and Biology

journal homepage: www.elsevier.com/locate/nucmedbio

Comparison of two new angiogenesis PET tracers ^{68}Ga-NODAGA-E[c(RGDyK)]$_2$ and ^{64}Cu-NODAGA-E[c(RGDyK)]$_2$; in vivo imaging studies in human xenograft tumors

Jytte Oxboel [a,*], Malene Brandt-Larsen [b], Christina Schjoeth-Eskesen [b], Rebecca Myschetzky [a,b], Henrik H. El-Ali [a], Jacob Madsen [b], Andreas Kjaer [a,b]

[a] Cluster for Molecular Imaging, Faculty of Health Sciences, University of Copenhagen, DK-2200 Copenhagen N, Denmark
[b] Department of Clinical Physiology, Nuclear Medicine & PET, Rigshospitalet, DK-2100 Copenhagen, Denmark

ARTICLE INFO

Article history:
Received 4 October 2013
Received in revised form 26 November 2013
Accepted 4 December 2013

Keywords:
Integrin $\alpha_v\beta_3$
RGD dimer
Angiogenesis
NODAGA
^{64}Cu
^{68}Ga
Cancer
Molecular imaging

ABSTRACT

Introduction: The aim of this study was to synthesize and perform a side-by-side comparison of two new tumor-angiogenesis PET tracers ^{68}Ga-NODAGA-E[c(RGDyK)]$_2$ and ^{64}Cu-NODAGA-E[c(RGDyK)]$_2$ in vivo using human xenograft tumors in mice. Human radiation burden was estimated to evaluate potential for future use as clinical PET tracers for imaging of neo-angiogenesis.

Methods: A ^{68}Ge/^{68}Ga generator was used for the synthesis of ^{68}Ga-NODAGA-E[c(RGDyK)]$_2$. ^{68}Ga and ^{64}Cu labeled NODAGA-E[c(RGDyK)]$_2$ tracers were administrated in nude mice bearing either human glioblastoma (U87MG) or human neuroendocrine (H727) xenograft tumors. PET/CT scans at 3 time points were used for calculating the tracer uptake in tumors (%ID/g), integrin $\alpha_v\beta_3$ target specificity was shown by blocking with cold NODAGA-E[c(RGDyK)]$_2$, and biodistribution in normal organs were also examined. From biodistribution data in mice human radiation-absorbed doses were estimated using OLINDA/EXM software.

Results: ^{68}Ga-NODAGA-E[c(RGDyK)]$_2$ was synthesized with a radiochemical purity of 89%–99% and a specific activity (SA) of 16–153 MBq/nmol. ^{64}Cu-NODAGA-E[c(RGDyK)]$_2$ had a purity of 92%–99% and an SA of 64–78 MBq/nmol.

Both tracers showed similar uptake in xenograft tumors 1 h after injection (U87MG: 2.23 vs. 2.31%ID/g; H727: 1.53 vs. 1.48%ID/g). Both RGD dimers showed similar tracer uptake in non-tumoral tissues and a human radiation burden of less than 10 mSv with an administered dose of 200 MBq was estimated.

Conclusion: ^{68}Ga-NODAGA-E[c(RGDyK)]$_2$ and ^{64}Cu-NODAGA-E[c(RGDyK)]$_2$ can be easily synthesized and are both promising candidates for PET imaging of integrin $\alpha_v\beta_3$ positive tumor cells. ^{68}Ga-NODAGA-E[c(RGDyK)]$_2$ showed slightly more stable tumor retention. With the advantage of in-house commercially ^{68}Ge/^{68}Ga generators, ^{68}Ga-NODAGA-E[c(RGDyK)]$_2$ may be the best choice for future clinical PET imaging in humans.

1. Introduction

Angiogenesis, the formation of new blood vessels, plays an important role in many pathological processes such as cancer. Integrin $\alpha_v\beta_3$ is a cell adhesion molecule and is highly expressed on activated endothelial cells and tumor cells, but not on resting endothelial cells. During the past decade many preclinical studies and clinical trials have confirmed the importance of integrin $\alpha_v\beta_3$ as a specific target for neo-angiogenesis, due to its role in the tumor growth and metastasis [1–3]. Extracellular matrix (ECM) proteins such as vitronectin, fibrinogen and fibronectin interact with integrin $\alpha_v\beta_3$ via the amino acid sequence Arg-Gly-Asp (RGD) [4–6]. Often reported RGD peptides used for radiolabeling are the cyclic pentapeptides cyclo(Arg-Gly-Asp-D-Phe-Lys), c(RGDfK) and cyclo(Arg-Gly-Asp-D-Tyr-Lys), c(RGDyK), which only differ with one amino acid [7–23]. Multimeric c(RGDxK) (x = y or f), as dimeric, tetrameric and octameric c(RGDxK), has been investigated to optimize the tracer uptake in integrin $\alpha_v\beta_3$ positive tumor cells. Affinity for integrin $\alpha_v\beta_3$ is enhanced and tracer uptake improves when peptide multiplicity increases, however also the tracer uptake in organs increases significantly, resulting in poor Tumor-to-Organ ratios. The conclusion is therefore that dimeric c(RGDxK) tracers may be the optimal choice with respect to tumor-to-Background ratios [19].

Cyclic RGD peptides targeting integrin $\alpha_v\beta_3$ in various tumor models and labeled with positron-emitting radionuclides (^{18}F, ^{68}Ga, ^{64}Cu) for positron emission tomography (PET) have been reported [7–23]. Several bifunctional chelators (BFC) such as 1,4,7,10-tetraazacyclododecane-N,N′,N″,N‴-tetraacetic acid (DOTA), 1,4,7-triazacyclononane-N,N′;N″-triacetic acid (NOTA) and 1,4,7-triazacyclononane-1-glutaric acid-4,7-diacetic acid (NODAGA) have been conjugated to RGD peptides, where NODAGA is particularly useful for ^{68}Ga- and ^{64}Cu-labeling due to high hydrophilicity and in vivo stability of its ^{68}Ga and ^{64}Cu chelates [19].

* Corresponding author: Tel.: +45 35 32 75 21; fax: +45 35 32 75 46.
E-mail address: joxbol@sund.ku.dk (J. Oxboel).

0969-8051
http://dx.doi.org/10.1016/j.nucmedbio.2013.12.003

The aim of the present study was to synthesize and make a side-by-side comparison of the two new tumor-angiogenesis PET tracers ^{68}Ga-NODAGA-E[c(RGDyK)]$_2$ and ^{64}Cu-NODAGA-E[c(RGDyK)]$_2$ using human glioblastoma (U87MG) and human neuroendocrine (H727) xenograft tumors in mice. We compared the tracer uptake of the ^{68}Ga- and ^{64}Cu-labeled NODAGA-E[c(RGDyK)]$_2$, for ^{68}Ga-tracer with "high" and "low" specific radioactivity, investigated the specificity of the dimeric c(RGDyK) by blocking with cold peptide, performed biodistribution studies, and estimated the radiation burden in humans by projecting radiation dosimetry data from mice.

2. Materials and methods

2.1. General

The 50 mCi ^{68}Ge/^{68}Ga generator was purchased from Eckert & Ziegler (Berlin, Germany) and was eluted with 0.1 N HCl (Biochemical grade; Fluka) using the fractionated elution approach. ^{64}CuCl$_2$ was produced at DTU-Risoe, Roskilde, Denmark [24]. NODAGA-c(RGDyK)$_2$ was purchased from ABX GmbH (advanced biochemical compounds, Radeberg, Germany). Sodium acetate, ammonium acetate and TraceSELECT water were purchased from Sigma-Aldrich. For high-performance liquid chromatography (HPLC) analysis a Dionex P580 pump with a PDA-100 detector and an in-line Scansys radioactivity detector was used. HPLC analysis was performed with a Jupiter 4u Proteo 90A, 250 × 4.6 mm (Phenomenex) and 1.5 mL/min flow. HPLC eluents were: A—90:10 (v/v) water: acetonitrile containing 0.1% trifluoroacetic acid; and B—90:10 (v/v) acetonitrile: water containing 0.1% trifluoroacetic acid. Gradient: 0–2 min 0% B, 2–7 min 40% B, and 7–9 min 0% B, 10 min 0% B.

2.2. Radiochemistry

2.2.1. ^{68}Ga-NODAGA-E[c(RGDyK)]$_2$ synthesis

^{68}Ga ($t_{1/2}$ = 68 min; $E_{max,\ \beta+}$ = 1.90 MeV (89%)) labeling was performed using the fractionated method [24]. The ^{68}Ge/^{68}Ga generator was eluted with 6 ml 0.1 N HCl into 6 tubes containing 1 ml each. The fraction with approximately 80% of the entire activity (1 ml, 450–500 MBq) was transferred to a vial containing 2 or 20 nmol NODAGA-E[c(RGDyK)]$_2$ acetate (Fig. 1) and 1 ml 0.7 M NaOAc buffer (pH 5.2). The reaction mixture was left at room temperature for 15 min, and the mixture was purified by C18 light SepPak. HPLC analysis of the final product revealed that the retention time of ^{68}Ga-NODAGA-E[c(RGDyK)]$_2$ was 6.3 min.

2.2.2. ^{64}Cu-NODAGA-E[c(RGDyK)]$_2$ synthesis

NODAGA-E[c(RGDyK)]$_2$ (2 nmol) was mixed with 450 μL ammonium acetate (0.1 M, pH 8.4), and 50 μL of ^{64}CuCl$_2$ (50–60 MBq) was added (^{64}Cu: $t_{1/2}$ = 12.7 h; $E_{max,\ \beta+}$ = 0.653 MeV (18%)). The solution was left at room temperature for 15 min. The product was used without further purification.

HPLC analysis of the final product revealed that the retention time of ^{64}Cu-NODAGA-E[c(RGDyK)]$_2$ was 6.5 min.

2.3. Cell lines and animal model

Human lung bronchus carcinoid, NCI-H727 and Human glioblastoma, U87MG both obtained from ATCC (American Type Culture Collection, Manassas, VA, USA) were used. Cell lines were tested free of Mycoplasma at the State Serum Institute, Copenhagen, Denmark before taking into experiments. H727 cells were cultured in RPMI (Roswell Park Memorial Institute) 1640 Medium with GlutaMAX™ (Gibco®, Life Technologies, NY, USA), U87MG in DMEM (Dulbecco's Modified Eagle Medium), high glucose, also with GlutaMAX™ (Gibco®, Life Technologies, NY, USA). Both cell lines were supplemented with 10% (v/v) fetal calf serum (Biological Industries (BI), Kibbutz Beit-Haemek, Israel) and 1% (v/v) penicillin–streptomycin (Gibco®, Life Technologies, NY, USA) in 5% CO_2 at 37°C.

Female NMRI (Naval Medical Research Institute) nude mice were acquired from Taconic Europe, Lille Skensved, Denmark. Xenografts of the two human cancer cell lines were established by injection of 100 μL medium containing 1 × 10^7 cells, suspended in 100 μL Matrixgel™ Basement Membrane Matrix (BD Sciences, San José, CA, USA) subcutaneously on the left and right flanks, under anesthesia with 1:1 V/V Hypnorm® (Janssen Pharmaceutica NV, Beerse, Belgium)/ Dormicum® (Roche, Basel, Switzerland). When reaching a tumor volume of approximate 100–300 mm^3 3–4 weeks after inoculation, the mice were enrolled in biodistribution, small animal PET/CT and blocking studies. All animal experiments were performed under the approval of the Danish Animal Welfare Council (2011/561-14).

2.4. Biodistribution studies

Mice were tail-vein injected with 4.4 ± 1.4 MBq (mean±SD) ^{68}Ga-NODAGA-E[c(RGDyK)]$_2$ or 5.2 ± 1.2 MBq ^{64}Cu-NODAGA-E[c(RGDyK)]$_2$ under sevoflourane anaesthesia. Biodistribution of ^{68}Ga-NODAGA-E[c(RGDyK)]$_2$ was obtained at 1, 2 and 4 h post injection (h pi), and of ^{64}Cu-NODAGA-E[c(RGDyK)]$_2$ at 1, 4 and 18 h pi (n = 4–6 mice in each group). Mice were sacrificed and major organs (liver,

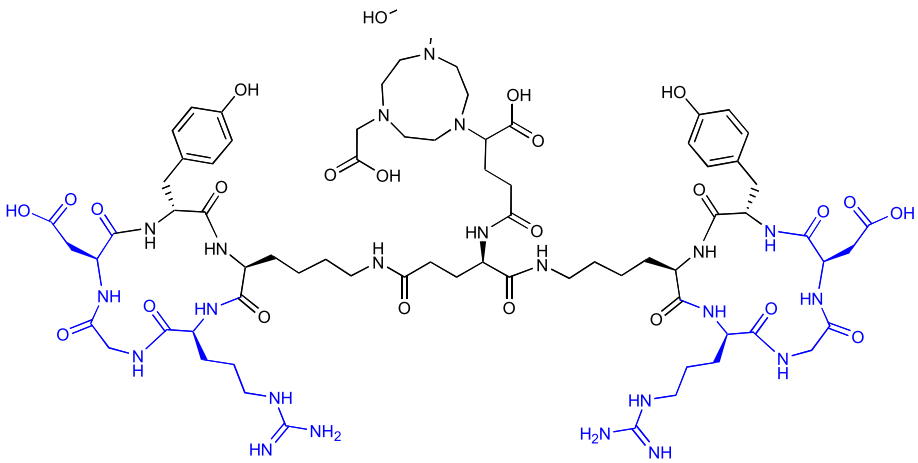

Fig. 1. Chemical structure of NODAGA-E[c(RGDyK)]$_2$.

kidneys, lung, spleen, heart, intestine, muscle) and blood were collected and wet-weighed. The radioactivity was measured using a gamma-counter (2480 Wizard®, Perkin Elmer, MA, USA). The results are presented as percentage of injected dose per gram tissue (%ID/g).

2.5. Small animal PET and CT

2.5.1. Imaging experiments

Mice bearing U87MG and H727 tumors were scanned statically with both ^{68}Ga- and ^{64}Cu-labeled NODAGA-E[c(RGDyK)]$_2$ containing 2 nmol of peptide. PET scans with ^{68}Ga-labeled tracer were performed 1, 2 and 4 h pi after tail-vein injection of 4.8 ± 0.9 MBq (mean±SD); regarding ^{64}Cu labeled tracer 1, 4 and 18 h pi with injection of 5.0 ± 1.0 MBq. Scan time was 15 and 20 min, respectively. n = 12–14 tumors for each xenograf tumor model at each scan time.

Preparations containing 20 nmol NODAGA-E[c(RGDyK)]$_2$ were also investigated with ^{68}Ga-labeling. PET/CT static scans 1, 2 and 4 h pi after injection of 4.9 ± 0.7 MBq (mean±SD) were performed on mice bearing H727 or U87MG xenograf tumors (n = 10 of each tumor type). The results are presented as percentage of injected dose per gram tissue (%ID/g), and compared to the tracer uptake found in mice (n = 12 of each tumor type) administrated with ^{68}Ga-NODAGA-E[c(RGDyK)]$_2$.

All PET scans were performed using a small animal PET scanner (MicroPET Focus 120, Siemens Medical Solutions, Knoxville, TN, USA). The energy window for the emission PET scans was set to 350–650 keV with a time resolution of 6 ns. The acquired emission dataset was stored in list mode format and post-processed to 2 bytes 128 × 144 × 32 sinograms. The emission sinograms were reconstructed using 3D Maximum a posteriori (MAP) algorithms resulting in 4 bytes 256 × 256 × 95 images with a zoom factor of 1.443 and a voxel size of 0.30 × 0.30 × 0.79 mm^3. Resolution of the PET scanner was 1.5 mm at center field of view. The emission sinograms were corrected for dead time and decay time, and the system calibrated to provide the quantification unity in Becquerel's per cubic centimeter (Bq/cc).

CT data were acquired using a small animal Computed Tomography System (MicroCAT® II, Siemens Medical Solutions, USA). The X-ray tube settings were voltage 60 kVp, current 500 μA, and exposure time 430 ms per projection. A set of 360 projections was used for a full 360 scan. To increase sensitivity and to reduce the size of the datasets, CT projections were binned by 4. The projections were reconstructed using COBRA real-time reconstruction algorithm with the Shepp–Logan filter into a 512 × 512 × 768 matrix with a voxel size of 0.092 × 0.092 × 0.092 mm^3 [25].

2.5.2. Image analysis

^{68}Ga- and ^{64}Cu-NODAGA-E[c(RGDyK)]$_2$ uptake in U87MG and H727 tumors was quantified using the image analysis software **I**nveon **R**esearch **W**orkplace (IRW; Siemens Medical Solutions, Malvern, PA, USA). 3D regions of interest (ROIs) were drawn on the fused PET/CT images intending to cover the whole tumor volume. For each ROI the mean tracer uptake was calculated as percentage of the injected dose per gram tissue (%ID/g) assuming a tissue density of 1 g/cm^3.

2.6. Blocking studies

Blocking studies were performed by tail-vein injection of 125 μg unlabeled NODAGA-E[c(RGDyK)]$_2$ (Molecular weight: 1707 g/mol; corresponding to 3 mg c(RGDyK)/kg body weight) 10 min before tracer injection. Mice bearing U87MG tumors were PET and CT scanned 1 h pi with either ^{68}Ga- or ^{64}Cu-labeled NODAGA-E[c(RGDyK)]$_2$ and afterwards sacrificed immediately (n = 8 tumors for each tracer). For calculations of the biodistribution blood, tumors and major organs were collected, wet-weighted and gamma counted. Results are presented as %ID/g and correlated to unblocked data (Fig. 7). %ID/g for tumors was calculated from the PET/CT scans drawing regions of interest using Inveon software.

2.7. Dosimetry projection for humans

For estimation of the human radiation dose for both ^{68}Ga- and ^{64}Cu-labeled NODAGA-E[c(RGDyK)]$_2$ mice biodistribution data were used. The mean activity in mice organs at 1, 2 and 4 h pi for ^{68}Ga- (n = 5 mice at each time point), and 1, 4 and 18 h pi for ^{64}Cu-labeled NODAGA-E[c(RGDyK)]$_2$ (n = 4 mice) was used to calculate Residence Times (Bq*h/Bq) for each organ. Using the percent kg/g method with mass extrapolation, 56.9 kg (female) and 73.7 kg (male), data were extrapolated to human dosimetry. To ensure a conservative estimate the dynamic bladder model values were set to: urinary elimination fraction 75% and void interval 5 h. Finally the **E**ffective **D**ose (ED) in mSv/MBq for both adult male and female was calculated. The **O**rgan **L**evel **IN**ternal **D**ose **A**ssessment/**EX**ponential **M**odeling software (OLINDA/EXM version 1.1; Vanderbilt University, Nashville, TN, USA) was used for all calculations [26].

2.8. Statistics

Data are presented as mean ± SEM unless otherwise stated. Two-sample unequal variance t-test was used. $P < 0.05$ was considered significant.

3. Results

3.1. Radiochemistry

NODAGA-E[c(RGDyK)]$_2$ (2, 4, 10 and 20 nmol) was labelled with $^{68}GaCl_3$ eluate to investigate the optimal radiolabelling conditions for ^{68}Ga- NODAGA-E[c(RGDyK)]$_2$ in terms of specific radioactivity and radiochemical yield (Fig. 2).

NODAGA-E[c(RGDyK)]$_2$ (2 nmol) was labeled with ^{68}Ga in 15 min at room temperature with a radiochemical purity of 89%–99% after SepPak purification and a specific radioactivity of 60 ± 13.7 MBq/nmol (mean ± SEM) (n = 12).

In separate experiments the radiochemical purity of ^{68}Ga-NODAGA-E[c(RGDyK)]$_2$ was determined to be >94% in buffer, plasma and in the final formulation 1, 2 and 4 h after incubation.

NODAGA-E[c(RGDyK)]$_2$ was labeled with ^{64}Cu in 15 min at room temperature with a radiochemical purity of 92%–99% and a specific radioactivity of 71.1 ± 7.0 MBq/nmol (mean ± SEM) (n = 8). The purity of ^{64}Cu-NODAGA-E[c(RGDyK)]$_2$ in buffer was 95% and 90% 1

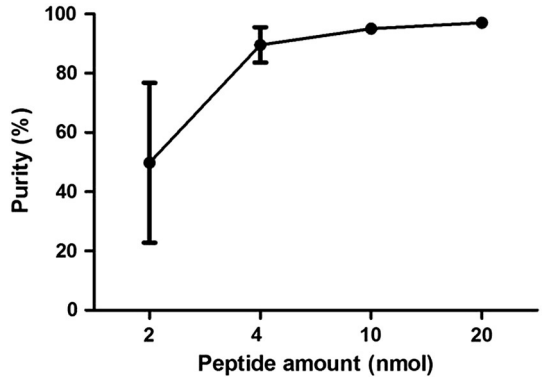

Fig. 2. Peptide amount versus radiochemical purity (before SepPak purification) for ^{68}Ga-NODAGA-E[c(RGDyK)]$_2$. The minimum amount of peptide practical possible to use was 2 nmol. Below 2 nmol the SepPak purification was unreliable. Using 4 nmol peptide higher and more reliable radiochemical yields were found. Data are shown as mean ± SD; 2 nmol: 49.8% ± 27.0% (n = 15); 4 nmol: 89.6% ±6.0% (n = 3); 20 nmol: 97.1% ± 0.4% (n = 4); for 10 nmol (n = 1).

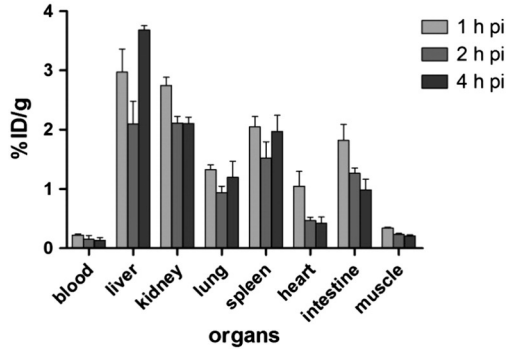

Fig. 3. Biodistribution data for ^{68}Ga-NODAGA-E[c(RGDyK)]$_2$ in mice 1, 2 and 4 h pi. Mice were tail-vein injected 4.4 ± 1.4 MBq (mean±SD) under sevoflourane anaesthesia. Results are shown as %ID/g (mean ± SEM).

and 2 days after incubation respectively. The purity in plasma was more than 96% 1, 2, 18, and 24 h after incubation.

3.2. Biodistribution data

For both tracers biodistribution in major organs (liver, kidneys, lung, spleen, heart, intestine, muscle) and blood was investigated, for ^{68}Ga-NODAGA-E[c(RGDyK)]$_2$ 1, 2 and 4 h pi, and for ^{64}Cu-NODAGA-E[c(RGDyK)]$_2$ 1, 4 and 18 h pi (n = 4–6 mice for each tracer). All tissues were gamma-counted 120 s and %ID/g calculated, corrected for counting-efficiency of the gamma-counter, tracer decay from injection to counting time, and tissue weight.

For ^{68}Ga-NODAGA-E[c(RGDyK)]$_2$ the highest tracer uptake in %ID/g (mean±SEM) was in liver 4 h pi (3.68±0.07) with an increase from 1 h pi (2.97 ± 0.39). For kidneys and intestines the highest tracer uptake was at 1 h pi (2.75 ± 0.14 and 1.82 ± 0.27) decreasing at 2 h pi (2.11 ± 0.11 and 1.27 ± 0.09) with further decrease for intestine (0.99 ± 0.18) but same level for kidneys (2.11 ± 0.10) at 4 h pi. Spleen had stable tracer accumulation during the measured time points (2.05 ± 0.18, 1.52 ± 0.28, and 1.97 ± 0.27) (Fig. 3).

For ^{64}Cu-NODAGA-E[c(RGDyK)]$_2$ the tracer uptake in all major organs was highest at 1 h pi decreasing over 4 h to 18 h pi. The highest %ID/g (mean±SEM) was found at 1 h pi for the kidneys, intestines, liver and spleen (3.12 ± 0.11, 1.61 ± 0.15, 1.31 ± 0.07, and 1.15 ± 0.06) decreasing at 4 h pi (1.80 ± 0.15, 1.15 ± 0.08, 1.19 ± 0.15, and 0.72 ± 0.01) and decreasing further at 18 h pi (1.02 ± 0.05, 0.98 ± 0.11, 0.99 ± 0.09, and 0.81 ± 0.06) (Fig. 4).

3.3. Small animal PET/CT

Both xenograft tumors were clearly visible on PET images for both NODAGA-E[c(RGDyK)]$_2$ tracers and easy to differentiate from non-tumoral tissues (Fig. 5).

For ^{68}Ga-NODAGA-E[c(RGDyK)]$_2$ the tracer uptake in tumor – in %ID/g (mean±SEM) – was highest in U87MG xenografts 1 h pi 2.23 ± 0.08. At 2 h pi the value was 2.02 ± 0.12 at, and at 4 h pi 1.93 ± 0.14 (n = 7-9 tumors). For H727 xenografts we also found the highest uptake 1 h after injection 1.53 ± 0.06, 1.39 ± 0.05 at 2 h pi, and declining significantly (P < 0.05) to 1.18 ± 0.12 at 4 h pi. For both xenograft tumor models we found an overall unchanged tracer uptake with no significant decrease at any time points except for H727 at 4 h pi compared to the level at 1 h pi (Fig. 6 A).

For ^{64}Cu-NODAGA-E[c(RGDyK)]$_2$ the tracer uptake was highest in U87MG tumors with 2.31 ± 0.15 at 1 h pi, 2.05 ± 0.14 at 4 h pi, and declining significantly (P < 0.001) to 0.52 ± 0.04 at 18 h pi (n = 12–14). For H727 tumors tracer uptake was 1.48 ± 0.08 at 1 h pi, and declining significantly at 4 and 18 h pi (P < 0.001) to 0.73 ± 0.04 and 0.54 ± 0.07 (Fig. 6 B). Tracer uptake for H727 was decreased significantly already at 4 h pi.

3.4. Specific radioactivity

The specific radioactivity of the ^{68}Ga labeled tracer using 2 nmol NODAGAE- NODAGA-E[c(RGDyK)]$_2$ was 60.7 ± 13.7 MBq/nmol (mean ± SEM) and 16.7 ± 0.3 MBq/nmol using 20 nmol peptide.

Tracer uptake 1 h pi in U87MG tumors in %ID/g (mean ± SEM) with 2 nmol peptide was 2.23 ± 0.08 (n = 9), and significantly (P < 0.001) lower for 20 nmol peptide 0.43 ± 0.04 (n = 10). Tracer uptake in H727 tumors as %ID/g (mean ± SEM) at same time point was 1.53 ± 0.06 (n = 10) and 0.32 ± 0.02 (P < 0.001) (n = 12). Similar results were seen for the PET scans at 2 and 4 h pi (Fig. 7 A-D).

In all the experiments in this study we used similar radioactivity of both tracers for injection in mice obtaining same, reliable counting statistic in the PET scans. Regarding similar specific activities of the tracers the mice were administrated with different amounts of peptid due to shorter half-life of ^{68}Ga and due to approximately one hour elapsed from end of synthesis. For ^{68}Ga-NODAGA-E[c(RGDyK)]$_2$ approximately twice as much peptide as with ^{64}Cu-NODAGA-E[c(RGDyK)]$_2$ (mean ± SD) 0.197 ± 0.073 nmol versus 0.083 ± 0.010 nmol) was therefore administered.

Using the calculated mean %ID/g of the ROI drawings of the PET/CT scans for both U87MG and H727 tumors, the Tumor-to-Organ ratios were calculated assuming good compliance between the two methods microPET and gamma-countering.

Tumor-to-Organ ratios using ^{68}Ga-NODAGA-E[c(RGDyK)]$_2$ tracer were similar for both xenograft tumor models; U87MG tumor-to-Muscle ratio was (mean±SEM) 6.6 ± 0.4 and H727 tumor-to-Muscle ratio was 4.6 ± 0.2 at 1 h pi. U87MG tumor-to-Blood ratio was 10.1 ± 0.8 1 h pi, increasing to 41.9 ± 12.5 2 h pi, compared to H727 tumor-to-Blood ratio of 6.5 ± 0.7 1 h pi and 28.8 ± 8.6 2 h pi (Table 1).

Tumor-to-Organ ratios for ^{64}Cu-NODAGA-E[c(RGDyK)]$_2$ tracer were quite similar to the ratios found for the ^{68}Ga-NODAGA-E[c(RGDyK)]$_2$ tracer: U87MG tumor-to-Muscle ratio was (mean±SEM) 6.7 ± 0.5, and H727 tumor-to-Muscle ratio 4.3 ± 0.3 at 1 h pi. The Tumor-to-Blood ratios were all at a higher level: U87MG tumor-to-Blood ratio was 23.4 ± 1.0 1 h pi, increasing to 128.5 ± 3.7 4 h pi, and H727 tumor-to-Blood ratio 15.0 ± 0.7 1 h pi and 45.7 ± 1.3 4 h pi (Table 2).

3.5. Blocking studies

The integrin $\alpha_V\beta_3$ receptor specificity of ^{68}Ga- and ^{64}Cu-labeled NODAGA-E[c(RGDyK)]$_2$ tracers was tested in a blocking study with administration of cold NODAGA-E[c(RGDyK)]$_2$, corresponding to approximately 3 mg c(RGDyK) per kg body weight, injected 10 min before the respective tracers. For ^{68}Ga-NODAGA-E[c(RGDyK)]$_2$ the tracer uptake in U87MG, calculated as %ID/g (mean±SEM) from the PET scans 1 h pi, was reduced significantly (P< 0.001) from 2.23 ± 0.08 (n = 9) to 0.20 ± 0.03 (n = 8), and for ^{64}Cu-NODAGA-E[c(RGDyK)]$_2$ reduced significantly (P< 0.001) from 2.31 ± 0.15 (n = 14) to 0.39 ±

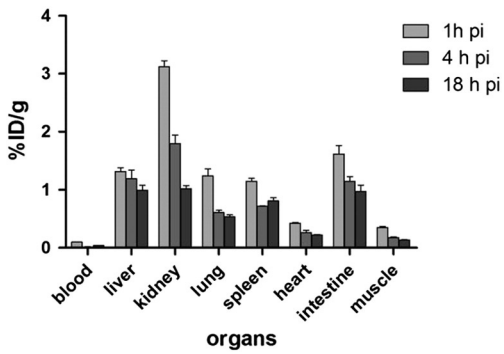

Fig. 4. Biodistribution data for ^{64}Cu-NODAGA-E[c(RGDyK)]$_2$ in mice 1, 4 and 18 h pi. Mice were tail-vein injected 5.2 ± 1.3 MBq (mean±SD) under sevoflourane anaesthesia. Results are shown as %ID/g (mean ± SEM).

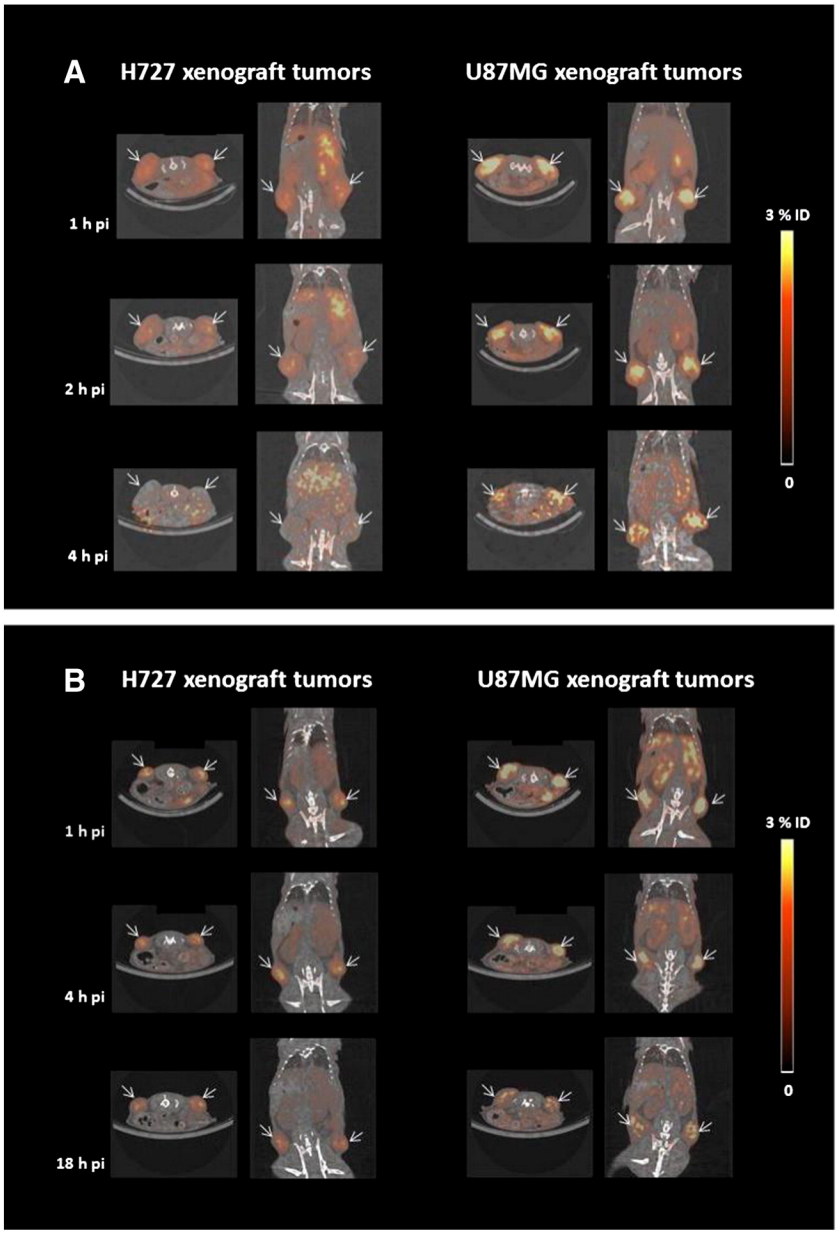

Fig. 5. PET/CT images of mice bearing U87MG or H727 xenograft tumors, A) Mice scanned for 15 min with 4.8 ± 0.9 MBq (mean±SD) ^{68}Ga-NODAGA-E[c(RGDyK)]$_2$ at 1, 2 and 4 h post injection, and B) Mice scanned for 20 min with 5.0 ± 1.0 MBq ^{64}Cu-NODAGA-E[c(RGDyK)]$_2$ at 1, 4, 18 h pi. Both coronal and axial slides are shown from a candidate mouse representing each tracer and tumor type. Tumors are marked with white arrows.

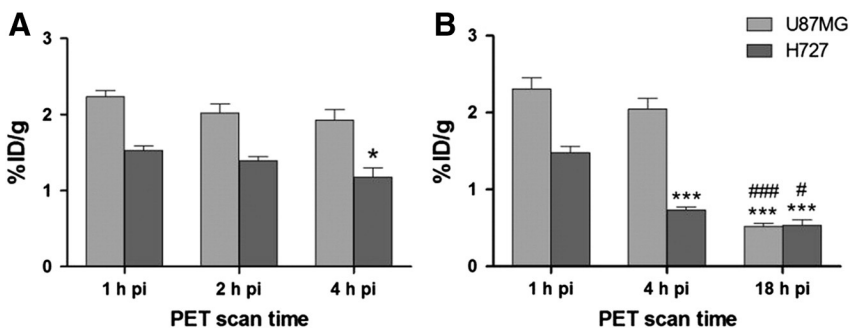

Fig. 6. A) ^{68}Ga-NODAGA-E[c(RGDyK)]$_2$ tracer uptake in U87MG and H727 xenograft tumor models. For H727 tumors a significant decreased tracer uptake was found from 1 to 4 h pi ($P < 0.05$). B) ^{64}Cu-NODAGA-E[c(RGDyK)]$_2$ tracer uptake in U87MG and H727 xenograft tumor models. For U87MG tumors a significant decreased tracer uptake was found from 1 to 18 h pi, and from 4 to 18 h pi (both $P < 0.001$). For H727 tumors a significant decreased tracer uptake was found from 1 to 4 h pi, from 1 to 18 h pi (both $P < 0.001$), and from 4 to 18 h pi ($P < 0.05$). Results are shown as %ID/g (mean±SEM).

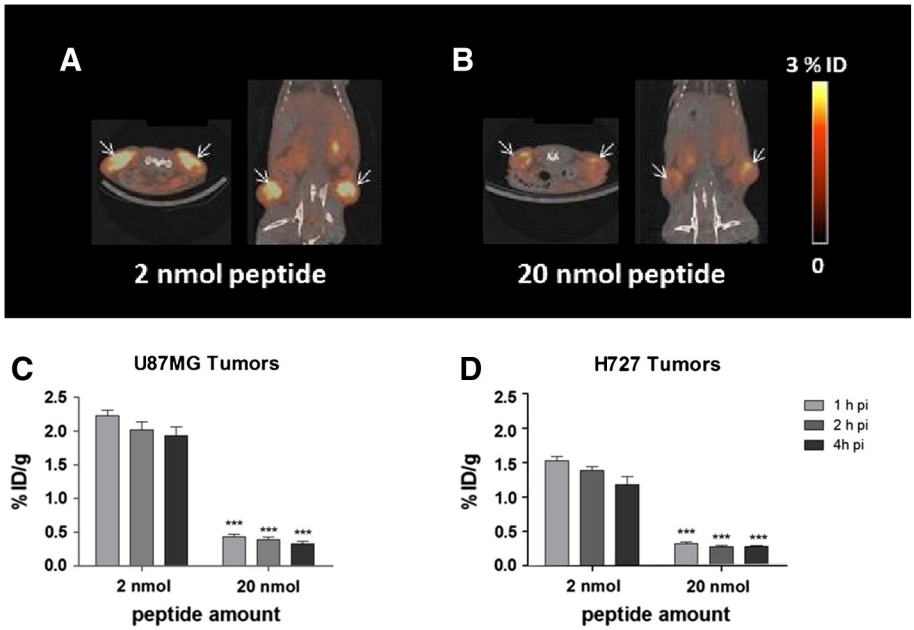

Fig. 7. Mice bearing human U87MG xenograft tumors (white arrows). PET scans were performed 1 h after injection of ^{68}Ga-NODAGA-E[c(RGDyK)]$_2$. A) 2 nmol NODAGA-E[c(RGDyK)]$_2$ used for labeling, resulting in a specific radioactivity of the tracer at 60.7 ± 13.7 MBq/nmol. B) 20 nmol NODAGA-E[c(RGDyK)]$_2$ used for labeling, resulting in a specific radioactivity of 16.7 ± 0.3 MBq/nmol. Tracer uptake in U87MG tumors (C) and H727 tumors (D) with ^{68}Ga-labeled tracer based on 2 or 20 nmol NODAGA-E[c(RGDyK)]$_2$ peptide. Results from PET scans at 1, 2 and 4 h post injection are shown in %ID/g (mean±SEM). ***): P < 0.001 for 2 versus 20 nmol peptide, at same time points and same xenograft tumor.

0.10 (n = 8) (Fig. 8 A and B). Administration of cold peptide also influenced the tracer uptake in all major organs showing a decreased tracer activity, except for ^{68}Ga-NODAGA-E[c(RGDyK)]$_2$ in liver where a 1.8 fold increase was observed (Fig. 8C and D).

3.6. Radiation Dosimetry

Residence times based on biodistribution data from both ^{68}Ga-NODAGA-E[c(RGDyK)]$_2$ and ^{64}Cu-NODAGA-E[c(RGDyK)]$_2$ tracers are shown in Table 3. Table 4 shows the calculated estimates of human radiation-absorbed doses using OLINDA/EXM, and the total effective doses (ED). The highest radiation-absorbed doses were found in the urinary bladder wall: for ^{68}Ga-NODAGA-E[c(RGDyK)]$_2$ 0.016 and 0.012 mGy/MBq for females and males, for ^{64}Cu-NODAGA-E[c(RGDyK)]$_2$ 0.020 and 0.015 mGy/MBq, respectively. This estimate was conservative because the dynamic bladder model values were set to a urinary elimination fraction of 75% and a void interval of 5 h. The whole body ED was for ^{68}Ga-NODAGA-E[c(RGDyK)]$_2$ 0.035 and 0.026 mSv/MBq for females and males, and for ^{64}Cu-NODAGA-E

Table 1
Tumor-to-Organ ratios for ^{68}Ga-NODAGA-E[c(RGDyK)]$_2$ at 1, 2 and 4 h pi; using U87MG and H727 xenograft tumors. Results are shown as mean ± SEM.

^{68}Ga-NODAGA-E[c(RGDyK)]$_2$						
Tumor-to-Organ Ratios						
	1 h pi		2 h pi		4 h pi	
	H727	U87MG	H727	U87MG	H727	U87MG
Tumor-to-blood	6.5 ± 0.7	10.1 ± 0.8	28.8 ± 8.6	41.9 ± 12.5	20.8 ± 7.2	34.0 ± 11.8
Tumor-to-liver	0.3 ± 0.1	0.8 ± 0.2	0.7 ± 0.1	1.1 ± 0.2	0.3 ± 0.00	0.5 ± 0.01
Tumor-to-kidney	0.6 ± 0.03	0.8 ± 0.04	0.7 ± 0.04	1.0 ± 0.05	0.6 ± 0.03	0.9 ± 0.05
Tumor-to-intestine	0.9 ± 0.2	1.4 ± 0.2	1.4 ± 0.2	2.0 ± 0.2	1.5 ± 0.4	2.5 ± 0.6
Tumor-to-Muscle	4.6 ± 0.2	6.6 ± 0.4	6.1 ± 0.4	8.9 ± 0.6	5.9 ± 0.5	9.6 ± 0.8

Table 2
Tumor-to-Organ ratios for ^{64}Cu-NODAGA-E[c(RGDyK)]$_2$ at 1, 4 and 18 h pi; using U87MG and H727 xenograft tumors. Results are shown as mean ± SEM.

^{64}Cu-NODAGA-E[c(RGDyK)]$_2$						
Tumor-to-Organ Ratios						
	1 h pi		4 h pi		18 h pi	
	H727	U87MG	H727	U87MG	H727	U87MG
Tumor-to-blood	15.0 ± 0.7	23.4 ± 1.0	45.7 ± 1.3	128.5 ± 3.7	14.9 ± 1.1	14.3 ± 1.1
Tumor-to-liver	1.1 ± 0.1	1.8 ± 0.1	0.7 ± 0.1	2.1 ± 0.1	0.6 ± 0.04	0.5 ± 0.04
Tumor-to-kidney	0.5 ± 0.02	0.8 ± 0.02	0.4 ± 0.03	1.3 ± 0.1	0.5 ± 0.03	0.5 ± 0.03
Tumor-to-intestine	0.9 ± 0.1	1.5 ± 0.1	0.6 ± 0.03	2.0 ± 0.1	0.6 ± 0.1	0.6 ± 0.1
Tumor-to-Muscle	4.3 ± 0.3	6.7 ± 0.5	4.2 ± 0.2	12.8 ± 0.5	4.1 ± 0.2	3.9 ± 0.2

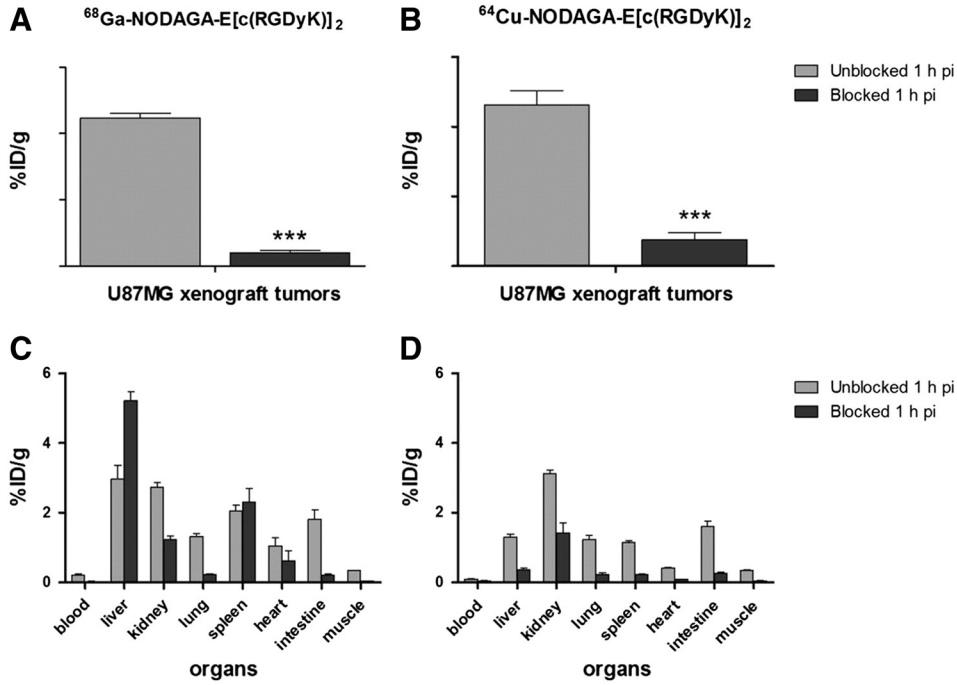

Fig. 8. Blocking with 3 mg c(RGDyK) per kg bodyweight followed by PET scan with ^{68}Ga-NODAGA-E[c(RGDyK)]$_2$ or ^{64}Cu-NODAGA-E[c(RGDyK)]$_2$. Tracer uptake: A) ^{68}Ga-NODAGA-E[c(RGDyK)]$_2$ and B) ^{64}Cu-NODAGA-E[c(RGDyK)]$_2$ in U87MG xenograft tumors with and without blocking with cold peptide. Results are shown as %ID/g (mean ± SEM), P 0.001. Tracer uptake: C) ^{68}Ga-NODAGA-E[c(RGDyK)]$_2$ and D) ^{64}Cu-NODAGA-E[c(RGDyK)]$_2$ in normal organs and blood with and without blocking with cold peptide. Results are shown as %ID/g (mean ± SEM).

[c(RGDyK)]$_2$ 0.050 and 0.039 mSv/MBq, respectively. Accordingly, an administered dose of 200 MBq ^{68}Ga-NODAGA-E[c(RGDyK)]$_2$ or ^{64}Cu-NODAGA-E[c(RGDyK)]$_2$ to humans would lead to an estimated radiation burden of 5.2 to 10 mSv (Table 4).

4. Discussion

Several RGD peptides labeled with isotopes for PET imaging have been proposed as useful ligands for integrin $\alpha_v\beta_3$ imaging [27–29]. The translation into clinic use of promising candidates such as ^{18}F-galacto-RGD has however been hampered by complicated multi-step radiochemistry difficult to automate [22]. Intense interest in developing radiolabelled RGD peptides conjugated to bifuntional chelators has therefore been pursued due to the simple radiolabelling procedures and availability of the radio metals.

In the present study we produced and evaluated two new PET tracers for imaging tumor neo-angiogenesis, and found promising imaging and dosimetry characteristics. The tracers are dimeric c(RGDyK) peptides conjugated with NODAGA and labeled with either ^{64}Cu or ^{68}Ga. Previous studies have shown high receptor-affinity to integrin $\alpha_V\beta_3$ for both c(RGDfK) and c(RGDyK)—the most often used RGD peptides for tracer labeling [7,8,10–17,20–23]. However c(RGDyK) shows higher tracer uptake in xenograft tumors probably due to the increased hydrophilicity of the D-Tyrosine (D-Tyr) compared to the D-Phenylalanine (D-Phe) derivative of c(RGDfK), and also faster renal excretion [8,16].

The affinity of c(RGDyK) or c(RGDfK) tracers targeting integrin $\alpha_V\beta_3$ is similar for both NODAGA- and DOTA-conjugated peptides, showing that the replacement of DOTA chelators with the NODAGA chelator has no influence on binding affinity or receptor specificity [11,15]. Advantages of NODAGA conjugated tracers are the increased Tumor-to Background and Tumor-to-Blood ratios with rapid renal excretion caused by higher hydrophilicity of NODAGA and high in vivo stability of both ^{68}Ga and ^{64}Cu chelates [15,19]. Studies with ^{68} Ga/^{64}Cu-labeled monomeric, dimeric, tetrameric or octameric RGD peptides showed increased receptor-binding affinity and specificity for integrin $\alpha_V\beta_3$, enhanced tumor uptake and longer tumor retention with increased numbers of RGD peptides, but also tracer accumulation in the kidneys, resulting in poorer Tumor-to-Kidney ratios [16,17]. Regarding Tumor-to-Background ratios there was no significant advantage in using radiolabeled tetrameric or octameric RGD peptides over the dimeric RGD peptides [19]. Thus dimeric RGD peptides were concluded to be the best candidates for further investigation for potential clinical translation. Initial attempts to synthesize ^{68}Ga-NODAGA-E[c(RGDyK)]$_2$ using the preconcentration approach where the ^{68}Ga-eluate is trapped on an ion exchange column and eluted with acetone/HCl mixture failed due to formation of large amounts of unknown biproducts. Therefore the fractionated approach [24] was tested and the radiolabelling was straightforward. To optimize the specific activity of ^{68}Ga-NODAGA-E[c(RGDyK)]$_2$ the labeling efficiency as a function of amount of precursor was also investigated (Fig. 2). To obtain optimal specific radioactivity 2 nmol of peptide was selected since lower amounts of peptide did not give reliable results. The relative large variation in the SA of ^{68}Ga-NODAGA-E[c(RGDyK)]$_2$ (16–153 MBq/nmol) is a consequence of the variation on the radiochemical yield.

Table 3
Residence times (Bq*h/Bq) in the main target organs for both ^{68}Ga-NODAGA-E[c(RGDyK)]$_2$ and ^{64}Cu-NODAGA-E[c(RGDyK)]$_2$. Data based on biodistribution in mouse organs.

Target Organ	Residence time (Bq*h/Bq)			
	^{68}Ga-NODAGA-RGD-dimér		^{64}Cu-NODAGA-RGD-dimér	
	Female	Male	Female	Male
Heart Wall	3.83E-03	3.90E-03	6.08E-03	6.13E-03
Kidneys	1.16E-02	9.76E-03	7.72E-02	6.48E-02
Liver	1.77E-01	1.33E-01	1.47E-01	1.53E-01
Lungs	7.98E-03	7.69E-03	5.14E-02	4.95E-02
Muscle	6.00E-02	7.36E-02	2.81E-01	3.59E-01
Small Intestine	1.01E-02	8.68E-03	6.65E-02	5.79E-02
Spleen	6.49E-03	6.11E-03	1.31E-02	1.22E-02
Remainder Body	1.49E + 00	1.49E + 00	1.73E + 01	1.70E + 01

Table 4
OLINDA estimated radiation-absorbed doses for human adults after injection of ^{68}Ga-NODAGA-E[c(RGDyK)]$_2$ and ^{64}Cu-NODAGA-E[c(RGDyK)]$_2$, respectively. Given a tracer dose of 200 MBq in patients, the radiation burden would be 5.2–6.9 mSv for ^{68}Ga-NODAGA-E[c(RGDyK)]$_2$, and 7.7–10.0 mSv for ^{64}Cu-NODAGA-E[c(RGDyK)]$_2$.

OLINDA estimated radiation-absorbed doses for human adults				
Taget Organ	Organ doses (mGy/MBq)			
	^{68}Ga-NODAGA-RGD-dimér		^{64}Cu-NODAGA-RGD-dimér	
	Adult female	Adult male	Adult female	Adult male
Adrenals	9.97E-05	7.58E-05	1.78E-04	1.37E-04
Brain	8.64E-05	7.00E-05	1.77E-04	1.42E-04
Breasts	8.04E-04	6.31E-04	1.56E-03	1.22E-03
Gallbladder Wall	0.00E + 00	0.00E + 00	0.00E + 00	0.00E + 00
Lower large Intestine Wall	2.65E-03	2.07E-03	5.15E-03	3.95E-03
Small Intestine	1.25E-04	1.04E-04	2.17E-04	1.84E-04
Stomach Wall	2.27E-03	1.78E-03	4.34E-03	3.42E-03
Upper large Intestine Wall	1.03E-04	8.07E-05	1.97E-04	1.54E-04
Heart Wall	0.00E + 00	0.00E + 00	0.00E + 00	0.00E + 00
Kidneys	1.28E-04	9.93E-05	1.63E-04	1.28E-04
Liver	3.41E-03	1.95E-03	8.65E-04	6.65E-04
Lungs	1.22E-03	9.16E-04	1.69E-03	1.32E-03
Muscle	3.85E-05	3.04E-05	6.49E-05	5.22E-05
Ovaries/Testes	4.33E-03	3.43E-03	8.32E-03	6.56E-03
Pancreas	4.73E-05	3.62E-05	7.10E-05	5.77E-05
Red Marrow	1.76E-03	1.44E-03	3.55E-03	2.84E-03
Osteogenic Cells	2.66E-04	1.98E-04	7.43E-04	5.52E-04
Skin	1.51E-04	1.19E-04	2.97E-04	2.31E-04
Spleen	1.26E-04	9.76E-05	8.55E-05	6.66E-05
Thymus	8.78E-05	6.70E-05	1.69E-04	1.28E-04
Thyroid	8.22E-04	6.68E-04	1.66E-03	1.33E-03
Urinary Bladder Wall	1.59E-02	1.19E-02	2.04E-02	1.53E-02
Uterus	1.24E-04	1.02E-04	2.29E-04	1.88E-04
Total Body	0.00E + 00	0.00E + 00	0.00E + 00	0.00E + 00
Effective Dose (mSv/MBq)	**3.46E-02**	**2.59E-02**	**5.01E-02**	**3.86E-02**
mSv, for 200 MBq dose	**6.92E + 00**	**5.18E + 00**	**1.00E + 01**	**7.72E + 00**

Radiosynthesis of ^{64}Cu-NODAGA-E[c(RGDyK)]$_2$ using 2 nmol peptide was straightforward giving robust results.

In the side-by-side comparison between ^{68}Ga-NODAGA-E[c(RGDyK)]$_2$ and ^{64}Cu-NODAGA-E[c(RGDyK)]$_2$ we found a similar tracer uptake in U87MG and H727 tumors (~2.3%ID/g and ~1.5%ID/g respectively) 1 h pi. The tracer retention was constant for both U87MG and H727 tumors with ^{68}Ga-NODAGA-E[c(RGDyK)]$_2$ over the time period from 1 to 4 h pi, and also for ^{64}Cu-NODAGA-E[c(RGDyK)]$_2$ in U87MG tumors from 1 to 4 h pi. For H727 tumors a decrease was found with both tracers from 1 to 4 h pi. When imaging at 18 h pi, only relevant for ^{64}Cu-NODAGA-E[c(RGDyK)]$_2$, decreased tracer uptake were found for both tumors (Fig. 5). More importantly, there was no increase in any of the Tumor-to-Organs ratio from 4 to 18 h pi making delayed imaging at 18 h unnecessary. In a previous study where we investigated ^{64}Cu-NODAGA-c(RGDyK), we also found a significant decrease in tracer uptake from 1 to 4 and 18 h pi in H727 xenograft tumors [21]. Tracer uptake of ^{68}Ga-NOTA- E[c(RGDyK)]$_2$ [17] showed similar tracer uptake in U87MG tumors (2.2%ID/g 1 h pi and 1.7%ID/g at 2 h pi) indicating that choice of chelator has no influence on the tracer uptake.

In the present study both dimeric NODAGA-E[c(RGDyK)]$_2$ tracers showed similar uptake in non-tumoral organs, with exception of a high ^{68}Ga- NODAGA-E[c(RGDyK)]$_2$ uptake in liver. A high uptake in liver is normally explained by higher hydrophobicity of the tracer resulting in rapid hepatobiliary excretion [14,18,22]. Apart from this exception the highest uptake in normal tissues was in the kidneys indicating the predominance of the renal excretion route. We found an increased kidney uptake for ^{64}Cu-NODAGA-E[c(RGDyK)]$_2$ compared to what we previously found for the monomeric RGD tracer ^{64}Cu-NODAGA-c(RGDyK) [21], resulting in minor but similar decreased Tumor-to-Kidney ratios for both investigated dimeric c(RGDyK) tracers. Mouse kidneys have high integrin $\alpha_V\beta_3$ expression on endothelial cells of small glomerulus vessels, indicating that the renal uptake of c(RGDxK) tracers is integrin $\alpha_V\beta_3$ specific. The increased kidney uptake from monomeric to dimeric c(RGDxK) can partly be explained by increased $\alpha_V\beta_3$-binding affinity [16]. An optimal radiotracer should, together with an early and high tumor uptake and a high tumor-to-background ratio, have a fast blood clearance. Regarding Tumor-to-Blood ratios ^{64}Cu-NODAGA-E[c(RGDyK)]$_2$ showed higher ratios than ^{68}Ga- NODAGA-E[c(RGDyK)]$_2$, but Tumor-to-Muscle (background) was similar for both dimeric c(RGDyK) tracers.

Effective blocking of integrin $\alpha_V\beta_3$ receptors with cold NODAGA-E[c(RGDyK)]$_2$ confirmed the specificity of the dimeric E[c(RGDyK)]$_2$ tracers in both U87MG and H727 xenograft tumors (Fig. 8).

In small animals, where the distribution volume is small, and the number of human receptors in xenograft tumors is limited, high SA is preferable in order to obtain high tracer uptake in tumors and sufficient contrast in PET images between target tissue and its surroundings [30]. In the literature SA of ^{68}Ga- and ^{64}Cu-c(RGDxK)-conjugates, varying from 10 to 550 MBq/nmol, reported all good tracer uptake in the tumors [12,15–17,21,22].

In the present study we investigated different levels of SA for ^{68}Ga-NODAGA-E[c(RGDyK)]$_2$ and found an SA of 60 MBq/nmol was sufficient for a high tracer uptake (>2% ID/g), whereas a lower SA (16 MBq/nmol) resulted in a significantly decreased tracer uptake (0.5% ID/g) which is unsuitable for imaging purposes (Fig. 7). Similar tracer uptake (>2%ID/g) was found for ^{64}Cu-NODAGA-E[c(RGDyK)]$_2$ with a specific activity of 71 MBq/nmol.

Taken together both ^{68}Ga-NODAGA-E[c(RGDyK)]$_2$ and ^{64}Cu-NODAGA-E[c(RGDyK)]$_2$ seem promising for future clinical use, with their individual specific advantages. We therefore performed estimates of dosimetry in humans based on projections from the mice data and found a favorable radiation burden of 10 mSv or less when administrated in a relevant dose of 200 MBq (Table 4).

5. Conclusion

^{68}Ga-NODAGA-E[c(RGDyK)]$_2$ and ^{64}Cu-NODAGA-E[c(RGDyK)]$_2$ are promising new candidates for PET imaging of integrin $\alpha_V\beta_3$ receptor

positive tumors. The two dimeric NODAGA-c(RGDyK) tracers showed higher integrin $\alpha_v\beta_3$ binding affinity compared to the monomeric NODAGA-c(RGDyK) tracers. Compared to ^{64}Cu-NODAGA-E[c(RGDyK)]$_2$, ^{68}Ga-NODAGA-E[c(RGDyK)]$_2$ showed a slightly more stable tumor retention for both U87MG and H727 xenograft tumors. Both tracers showed favorable human radiation burden estimates of less than 10 mSv calculated for a realistic clinical dose of 200 MBq.

Due to the better tumor retention and advantage of in-house commercially available ^{68}Ge/^{68}Ga generators, ^{68}Ga-NODAGA-E[c(RGDyK)]$_2$ may be the most promising candidate for clinical translation into humans for PET imaging neo-angiogenesis in many common cancer types.

Acknowledgments

The National Advances Technology Foundation, Danish Cancer Society, The Lundbeck Foundation, Novo Nordic Foundation, The Danish Medical Research Council, Svend Andersen Foundation, Research Council for Strategic Research, Rigshospitalets Research Council, the Arvid Nilsson Foundation, the John and Birthe Meyer Foundation, and A.P. Moeller Foundation supported this work.

Great thanks to Linda Magnusson for technical assistance with the tumor cell handling.

References

[1] Guo W, Giancotti FG. Integrin signalling during tumour progression. Nat Rev Mol Cell Biol 2004;5:816–26.
[2] Liu Z, Wang F, Chen X. Integrin alpha(v)beta(3)-targeted cancer therapy. Drug Dev Res 2008;69:329–39.
[3] Millard M, Odde S, Neamati N. Integrin targeted therapeutics. Theranostics 2011;1:154–88.
[4] Dijkgraaf I, Beer AJ, Wester HJ. Application of RGD-containing peptides as imaging probes for alphavbeta3 expression 2 2907. Front Biosci 2009;14:887–99.
[5] Ruoslahti E. RGD and other recognition sequences for integrins. Annu Rev Cell Dev Biol 1996;12:697–715.
[6] Ruoslahti E, Pierschbacher MD. New perspectives in cell adhesion: RGD and integrins. Science 1987;238:491–7.
[7] Buchegger F, Viertl D, Baechler S, Dunet V, Kosinski M, Poitry-Yamate C, et al. 68Ga-NODAGA-RGDyK for alphavbeta3 integrin PET imaging. Preclinical investigation and dosimetry. Nuklearmedizin 2011;50:225–33.
[8] Chen X, Liu S, Hou Y, Tohme M, Park R, Bading JR, et al. MicroPET imaging of breast cancer alphav-integrin expression with 64Cu-labeled dimeric RGD peptides. Mol Imaging Biol 2004;6:350–9.
[9] Chen X, Tohme M, Park R, Hou Y, Bading JR, Conti PS. Micro-PET imaging of alphavbeta3-integrin expression with 18 F-labeled dimeric RGD peptide. Mol Imaging 2004;3:96–104.
[10] Decristoforo C, Hernandez Gonzalez I, Carlsen J, Rupprich M, Huisman M, Virgolini I, et al. 68Ga- and 111In-labelled DOTA-RGD peptides for imaging of alphavbeta3 integrin expression. Eur J Nucl Med Mol Imaging 2008;35:1507–15.
[11] Dijkgraaf I, Terry SY, McBride WJ, Goldenberg DM, Laverman P, Franssen GM, et al. Imaging integrin alpha-v-beta-3 expression in tumors with an 18 F-labeled dimeric RGD peptide. Contrast Media Mol Imaging 2013;8:238–45.
[12] Dumont RA, Deininger F, Haubner R, Maecke HR, Weber WA, Fani M. Novel (64)Cu- and (68)Ga-labeled RGD conjugates show improved PET imaging of alpha(nu)beta(3) integrin expression and facile radiosynthesis. J Nucl Med 2011;52:1276–84.
[13] Ferl GZ, Dumont RA, Hildebrandt IJ, Armijo A, Haubner R, Reischl G, et al. Derivation of a compartmental model for quantifying 64Cu-DOTA-RGD kinetics in tumor-bearing mice. J Nucl Med 2009;50:250–8.
[14] Jeong JM, Hong MK, Chang YS, Lee YS, Kim YJ, Cheon GJ, et al. Preparation of a promising angiogenesis PET imaging agent: 68Ga-labeled c(RGDyK)-isothiocyanatobenzyl-1,4,7-triazacyclononane-1,4,7-triacetic acid and feasibility studies in mice. J Nucl Med 2008;49:830–6.
[15] Knetsch PA, Petrik M, Griessinger CM, Rangger C, Fani M, Kesenheimer C, et al. [68Ga]NODAGA-RGD for imaging alphavbeta3 integrin expression. Eur J Nucl Med Mol Imaging 2011;38:1303–12.
[16] Li ZB, Cai W, Cao Q, Chen K, Wu Z, He L, et al. (64)Cu-labeled tetrameric and octameric RGD peptides for small-animal PET of tumor alpha(v)beta(3) integrin expression. J Nucl Med 2007;48:1162–71.
[17] Li ZB, Chen K, Chen X. (68)Ga-labeled multimeric RGD peptides for microPET imaging of integrin alpha(v)beta (3) expression. Eur J Nucl Med Mol Imaging 2008;35:1100–8.
[18] Liu S. Radiolabeled multimeric cyclic RGD peptides as integrin alphavbeta3 targeted radiotracers for tumor imaging. Mol Pharm 2006;3:472–87.
[19] Liu S. Radiolabeled cyclic RGD peptides as integrin alpha(v)beta(3)-targeted radiotracers: maximizing binding affinity via bivalency. Bioconjug Chem 2009;20:2199–213.
[20] Liu Z, Li ZB, Cao Q, Liu S, Wang F, Chen X. Small-animal PET of tumors with (64)Cu-labeled RGD-bombesin heterodimer. J Nucl Med 2009;50:1168–77.
[21] Oxboel J, Schjoeth-Eskesen C, El-Ali HH, Madsen J, Kjaer A. (64)Cu-NODAGA-c(RGDyK) is a promising new angiogenesis PET tracer: correlation between tumor uptake and integrin alpha(V)beta(3) expression in human neuroendocrine tumor xenografts. Int J Mol Imaging 2012;2012 [379807].
[22] Pohle K, Notni J, Bussemer J, Kessler H, Schwaiger M, Beer AJ. 68Ga-NODAGA-RGD is a suitable substitute for (18)F-Galacto-RGD and can be produced with high specific activity in a cGMP/GRP compliant automated process. Nucl Med Biol 2012;39:777–84.
[23] Wu Y, Zhang X, Xiong Z, Cheng Z, Fisher DR, Liu S, et al. microPET imaging of glioma integrin {alpha}v{beta}3 expression using (64)Cu-labeled tetrameric RGD peptide. J Nucl Med 2005;46:1707–18.
[24] Thisgaard H, Jensen M, Elema DR. Medium to large scale radioisotope production for targeted radiotherapy using a small PET cyclotron. Appl Radiat Isot 2011;69:1–7.
[25] Binderup T, El-Ali HH, Ambrosini V, Skovgaard D, Jensen MM, Li F, et al. Molecular imaging with small animal PET/CT. Curr Med Imaging Rev 2011;7:234–47.
[26] Stabin MG, Sparks RB, Crowe E. OLINDA/EXM: the second-generation personal computer software for internal dose assessment in nuclear medicine. J Nucl Med 2005;46:1023–7.
[27] Cai HC, Conti PS. RGD-based PET tracers for imaging receptor integrin $\alpha v\beta 3$ expression. J Label Compd Radiopharm 2013. http://dx.doi.org/10.1002/jlcr.2999.
[28] Haubner R, Beer AJ, Wang H, Chen X. Positron emission tomography tracers for imaging angiogenesis. Eur J Nucl Med Mol Imaging 2010. http://dx.doi.org/10.1007/s00259-010-1503-4.
[29] Beer AJ, Kessler H, Wester HJ, Schwaiger M. PET imaging of integrin alphaVbeta3 expression. Theranostics 2011;1:48–57.
[30] Velikyan I, Beyer GJ, Bergstrom-Pettermann E, Johansen P, Bergstrom M, Langstrom B. The importance of high specific radioactivity in the performance of 68Ga-labeled peptide. Nucl Med Biol 2008;35:529–36.